DYNAMIC NUMERICAL STUDY ON PHASE CHANGE THERMAL STORAGE HEAT TRANSFER

by

Jie CUI[a*], Guofeng WANG[b], Zhitang GUO[a], Shuo YANG[b], Honggang PAN[a], Jianjun SHI[c], and Youning XU[b]

[a]School of Energy and Power, Shenyang Institute of Engineering, Shenyang, China
[b]Key Laboratory of Clean Combustion for Power Generation and Heat-Supply Technology of Liaoning Province, Shenyang Institute of Engineering, Shenyang, China
[c]State Power Investment Corporation Northeast Electric Power Co., Ltd., Shenyang, China

Original scientific paper
https://doi.org/10.2298/TSCI2106171C

Targeted at the poor heat transfer effect of the phase change thermal storage heat exchanger due to the low thermal conductivity of the phase change material, a fin-tube type phase change thermal storage heat exchanger has been proposed in the study. A 2-D model of the phase-change heat storage unit was established, and the dynamic heat transfer law of the melting and solidification of the phase change material, and the influence of the fin structure size on the heat storage/release performance of the heat exchanger were numerically analyzed. The results show that in the area close to the tube wall, the smaller the fin spacing, the larger the thickness, the faster the phase change heat storage/ release speed, and the better heat transfer effect. In the central area of the phase change material, the greater the fin spacing and thickness, and the better the heat transfer effect of the phase change heat storage/release. The area close to the outer wall has the smallest temperature change, and the heat storage/release effect is the worst. Therefore, the use of energy storage heat exchangers with gradual fin thickness and spacing is an effective method to improve the heat transfer efficiency of existing equipment. In addition, in order to improve the heat exchange effect of the edge area of the phase change, its structure could be changed or the heat exchange form can be increased.

Key words*: phase change thermal storage, fin spacing, fin thickness, melting, solidification*

Introduction

Phase change thermal storage technology is an effective way for energy conservation and emission reduction and can help rationally use energy. However, due to the low thermal conductivity of most phase change materials (PCM), the heat exchange efficiency is low in the phase change heat storage system, so there is an urgent need to carry out research on the performance enhancement of the phase change heat storage system [1-3].

*Corresponding author, e-mail: cuicuijiejie25@163.com

Li *et al*. [4] conducted an experimental study on the heat storage model of the finned convergent tube. According to the results, the heat transfer rate of the fin convergent tube (fin thickness of 2 mm) in the heat storage/heat release stage is 13% higher than that of the bare tube convergent tube. Increasing the thickness of the fin to a moderate extent can improve the heat storage and release performance of the heat storage body. Mat *et al*. [5] and Al-Abidi [6] established a 2-D numerical model to simulate the melting and solidification process in a triple spiral tube phase change heat accumulator with inner and outer fins, and studied the influence of different structural parameters on melting and the solidification process. Tao *et al.* [7] numerically studied the feasibility of using an enhanced heat transfer tube with internal fins to enhance the performance of a double-pipe phase change heat storage unit, and proved that enhancing the heat transfer performance on the heat transfer fluid side also is an effective way to improve the overall heat storage performance. Ismail *et al.* [8] established a ribbed mathematical model and found that the number, height and spacing of fins greatly affect the heat storage and energy storage.

In this paper, the dynamic numerical simulation analysis method is adopted to simulate the dynamic changes of the melting and solidification of the PCM in different regions during the heat storage and heat release process of the fin-tube heat exchanger. Furthermore, the influence of different fin structure sizes on phase change heat transfer have been compared and analyzed, and a reference has been provided for the design of fin type phase change energy storage heat exchangers.

Models and methods

Physical model

Figure 1 shows the physical model of the fin-tube phase-change energy storage heat exchanger. In this model, the PCM is used to fill the adjacent fins, and the heat transfer fluid flows into the middle heat exchange tube from top to bottom and exchanges heat with the PCM through the tube wall and fins of the heat exchange tube. This paper selects three typical measuring points in the phase change area: Measuring point 1 is close to the wall of the heat exchange tube, Measuring point 2 is located at the center of the phase change area, and Measuring point 3 is located at the farthest area from the heat exchange tube in the same radial direction of the phase change area. In this paper, the overall geometric parameters of the thermal storage unit set based on the experimental model parameters in [9, 10]. Please check tab. 1 for details.

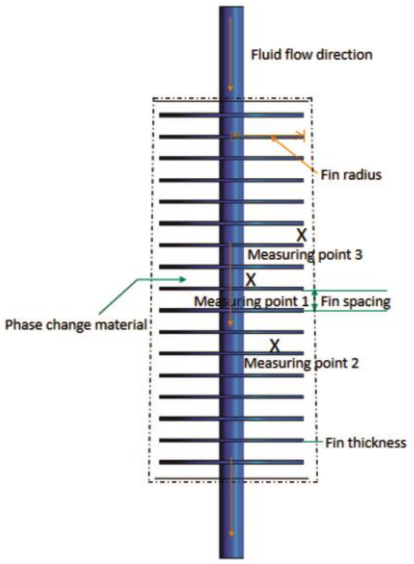

Figure 1. Physical model

Table 1. Geometric parameters of heat storage unit

Geometric parameters of thermal storage unit	Value
Fin thickness, δ [mm]	2, 4, 6
Fin spacing, d [mm]	16, 24, 32
Fin radius, r [mm]	45

Controlling equation

In order to establish the controlling equation of the system, this thesis assumes:

– A 1-D distributed parameter model is adopted for the heat transfer fluid, and the axial heat conduction and viscous dissipation of the heat transfer fluid are neglected.
– The flow of liquid PCM is unsteady, laminar and incompressible, which obeys Fourier heat conduction law [11].
– The thermal resistance of the inner tube wall of the phase change heat storage unit is neglected, and the surface of the outer tube should be isothermally treated.
– The density of the PCM accords with Boussinesq [12, 13].

The solidification/melting model in the commercial software FLUENT is used for numerical simulation, so the solid phase and liquid phase energy equations are established. The controlling equations for the system are shown:

$$\frac{\partial u}{\partial x}+\frac{\partial v}{\partial y}=0 \tag{1}$$

$$\frac{\partial(\rho u)}{\partial t}+\mathrm{div}(\rho u u)=\mathrm{div}(\mu \mathrm{grad} u)-\frac{\partial P}{\partial x}+S_x \tag{2}$$

$$\frac{\partial(\rho v)}{\partial t}+\mathrm{div}(\rho u v)=\mathrm{div}(\mu \mathrm{grad} v)-\frac{\partial P}{\partial y}+S_y \tag{3}$$

$$\frac{\partial \rho h_s}{\partial t}+\mathrm{div}(\rho u h_s)=\mathrm{div}\left(\frac{k}{c}\mathrm{grad} h_s\right)-S_h \tag{4}$$

where ρ is the density, μ – the dynamic viscosity, P – the pressure, k – the thermal conductivity, T_w – the hot surface temperature, u and v are the velocity components on the x-axis and y-axis, respectively, and S_x and S_y are the source term of the fuzzy area, respectively. Percentage of liquid β is introduced during calculation [14]. It is defined:

$$\beta\begin{cases}\dfrac{\Delta H}{L}=0, & T\le T_s\\ \dfrac{\Delta H}{L}=1, & T\ge T_1\\ \dfrac{\Delta H}{L}=\dfrac{T-T_s}{T_1-T}, & T_s\le T\le T_1\end{cases} \tag{5}$$

A solid-liquid mixing region (mush region) is defined in solidification/melting model between liquid phase and solid phase, and momentum equations of three different phases are solved by source term, S, which is defined:

$$S=\frac{c(1-\beta^2)}{\beta^2}\rho u \tag{6}$$

Additional explanations are the solid thermal conductivity, λ, is used when solving the solid domain, and the melting thermal conductivity, λ_{moze}, is used when solving the molten area. When solving the liquid area, the sum of convective thermal conductivity and thermal conductivity ($\lambda_f + h$) is used.

Result analysis

Comparison of numerical results and experimental data

According to the established physical and mathematical model, the mathematical model is divided by a full six-sided grid after verification of grid independence and time step. The time step is set to 5 seconds and the number of grids is 560000. Figure 2 is the grid diagram of the numerical model. In order to improve the calculation accuracy and ensure the calculation accuracy, the grid is encrypted and the grid independence is verified. Then, the correctness of the model and simulation program is verified by comparing with the experimental results in Dai *et al*. [9]. As shown in fig. 3, the experimental data (green curve) at the experimental Test Point 1 in [9] and the numerical calculation results (red curve) in this paper are selected for comparison and analysis.

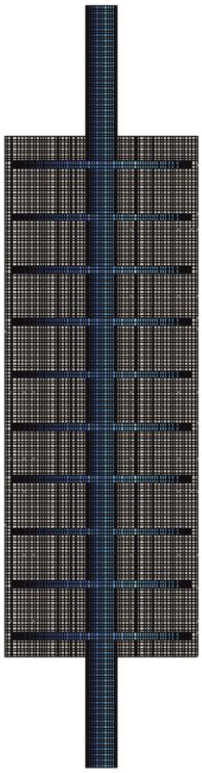

Figure 2. Mesh of numerical model

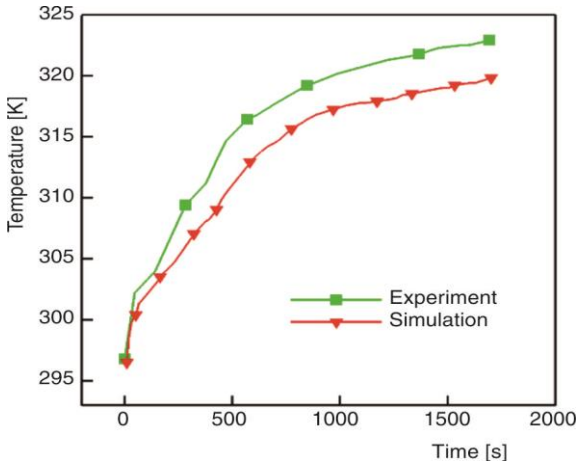

Figure 3. Temperature changes with time at Test Point 1

From fig. 3, the temperature curve of the numerical simulation is lower than that of the experiment because the wall of the numerical simulation cylinder is under isothermal conditions and the experimental cylinder wall uses adiabatic conditions. This leads to an increase in the heat exchange between the outer wall and the outside of the numerical simulation calculation result, and the system temperature decreases, so the curve numerical simulation result is lower than that of experimental result. However, it can be found from fig. 3 that temperature change trajectory of the two is roughly similar, and the numerical difference is also small, which indicates that the numerical simulation method can be used for detailed analysis of other problems.

Comparative analysis of heat transfer capacity of different structures

The heat exchange structures with different fin spacings of 16 mm, 24 mm, 32 mm, and different fin thicknesses of 2 mm, 4 mm, 6 mm are selected to analyze the relationship between the temperature of different observation points and time in the phase transition area

of the fins. As shown in fig. 4, there are a total of 9 curves, which represent the melting (heat storage) and solidification (heat release) process curves at three measuring point in the phase change area. The legend curve p-1-16-2 shows the relationship between time and the temperature of the fin at the measuring point 1-the pitch of 16 mm-the fin thickness of 2 mm, and the meanings of other curves can be deduced by analogy.

- A (3690, 344), B (3890, 341), C (3010, 339) the highest point of the melting stage of measuring Point 1.
- D (3010, 326), E (3890, 326), F (3650, 320) measuring Point 2 the highest point of the melting stage.
- G (970, 316), H (2510, 317) measuring Point 3 the highest point of melting stage.
- J (3410, 305), K (4370, 304), I (3970, 302) measuring Point 1 changed from the melting process to the starting point of the solidification process.

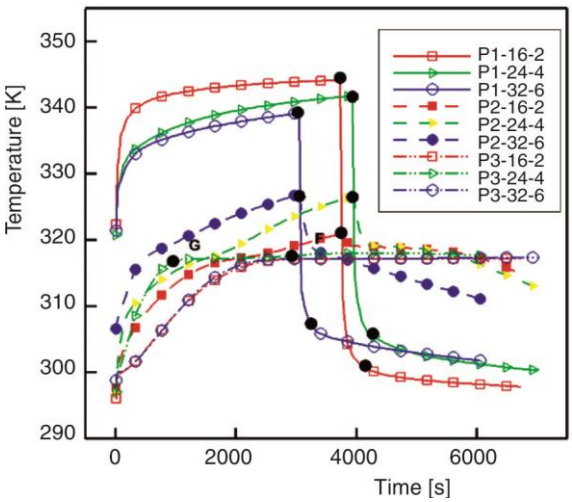

Figure 4. The relationship between temperature and time under different working conditions

It can be seen from fig. 4 that when t = 2000 seconds, the temperature of the phase transition area of the fin with a distance of 16 mm and a thickness of 2 mm on the curve of measuring Point 1 is 343 K, and the temperature of the phase transition area of the fin with a distance of 24 mm and a thickness of 4 mm is 339 K, the temperature in the phase transition zone of the fin with a pitch of 32 mm and a thickness of 6 mm is 336.5 K. The results show that the temperature in the phase transition zone of the fin with a spacing of 16 mm is significantly higher than the temperature in the phase transition zone of the other two fins with a spacing. The P-1-16-2 curve is also the highest of all the curves, which shows that for the area close to the wall of the heat exchange tube, the small spacing and thickness of the fin structure is beneficial to the rapid melting of the phase change area.

From the numerical simulation results of the heat storage process and heat release process of different structures, it can be concluded that in the phase change area close to the heat exchange center tube, the smaller the fin spacing, the thinner the thickness, the faster the heat storage and heat release, and the better heat exchange effects. In the central area of the phase change medium, the larger the fin spacing, the thicker the structure has a better heat transfer effect. The phase change area near the outer wall is the most difficult place to store heat and the minimum temperature change area.

Analysis of phase transition temperature change process

The melting process of the PCM area can be divided into four stages, *i.e.*, the initial heating period, the smooth phase change period, the accelerated heating period, and the temperature saturation period. The temperature change of the fin area undergoes three stages of rapid heating, gentle temperature and slow heating [12, 15]. Numerical methods can be used to analyze the temperature change process in the different stages, and observe the temperature

change of each point in the phase change area with time, which can better explain the influence of the structure size on the PCM.

Figure 5 shows the temperature distribution of the phase change medium at different moments calculated for the heat storage with spacing of 24 mm and a thickness of 4 mm. It can be seen from the figure that when t = 10 seconds, the temperature of the PCM near the heat exchange tube is 304 °C, the melting process do not started, and the temperature do not reach the lowest temperature of melting of the PCM. When t = 170 seconds, the temperature distribution is obviously stratified, the color gradually darkens from the center to the edge, and the PCM at the edge does not start to melt at a temperature of 300 °C. When t = 810 seconds, the PCM close to the heat exchange tube begins to melt, and the temperature extends in the diameter of the PCM. The edge part is in a state of solid-liquid coexistence or a solid phase state. When t = 2010 seconds, the melting process proceeds further, and the temperature of the edge part reaches 315 °C, and the PCM turns from solid state to liquid gradually. When t = 3890 seconds, the melting part reaches the maximum, the PCM near the heat exchange tube reaches the highest temperature of 350 °C. Since then, the melting process is coming to an end. When t = 4250 seconds, cold water is injected, the solidification process begins, a and the PCM near the heat exchange tube is melting. The material starts to solidify at a temperature of 298 °C, and other parts are in a state of solid-liquid coexistence. When t = 5010 seconds, the solidification process further occurs and stratification occurs. When t = 6610 seconds, the part of the solidification area near the heat exchange tube increases and the rest is in constant solidification.

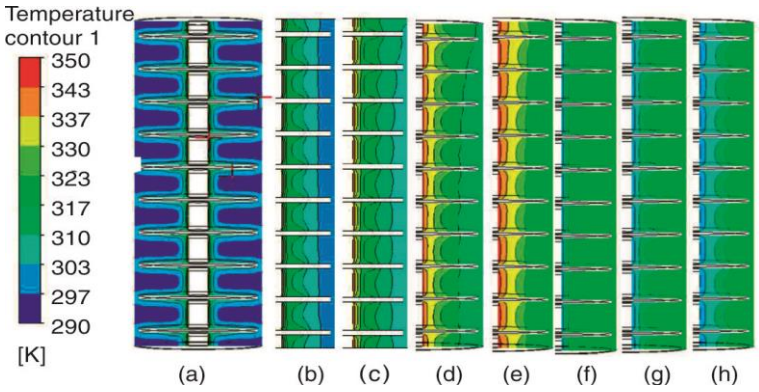

Figure 5. Change of temperature with time during phase transition; (a) t = 10 seconds initial time, (b) t = 170 seconds initial heating period, (c) t = 810 seconds phase transition flat period, (d) t = 2010 seconds heating period, (e) t = 3890 seconds temperature saturation period, (f) t = 4250 seconds solidification process, (g) t = 5010 seconds solid-liquid coexistence state, and (h) t = 6610 seconds solidification process

Analysis of the change process of liquid mass fraction

The phase change process of the solid-liquid term can describe the heat exchange process and heat exchange effect of the finned heat storage. Figure 6 shows the distribution of liquid mass fraction with time obtained from numerical simulation of heat storage with spacing of 24 mm and thickness of 4 mm. It can be seen from the figure that at the initial time t = 10 seconds, there is a solid phase in the pipe. When t = 610 seconds, liquid phase begins to precipitate near the central area of the pipe. As time progresses, the volume of the

liquid phase increases in the radial direction. When t = 3050 seconds, the volume of the liquid phase in the system is relatively large. When t = 4250 seconds, the system enters the solidification state, the system begins to solidify and release heat, and the central area begins to transform from the liquid phase to the solid phase. With the increase of time, the volume of solid phase increases, but the solidification speed is slow in the part far away from the central tube. When t = 7010 seconds, there will be no solidification in the area near the wall where solid and liquid coexist. This phenomenon is a typical problem existing in this type of fin heat exchanger.

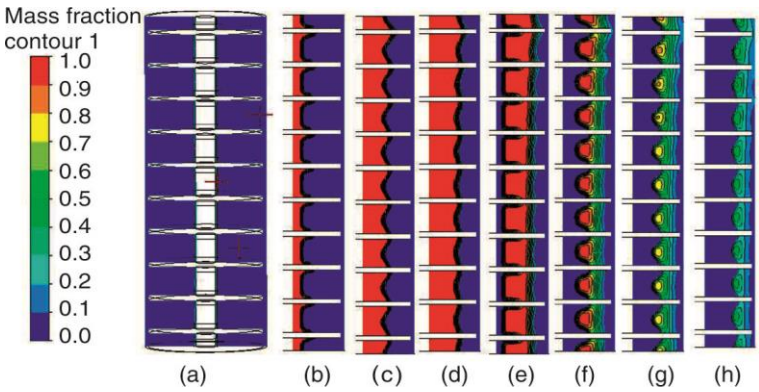

Figure 6. Change of temperature mass fraction with time during phase transition; (a) t = 10 seconds initial time, (b) t = 610 seconds phase transition flat period, (c) t = 2050 seconds heating period, (d) t = 3050 seconds heating period, (e) t = 4250 seconds solidification process, (f) t = 5050 seconds solid-liquid coexistence state, (g) t = 6010 seconds solidification process, and (h) t = 7010 seconds solidification process

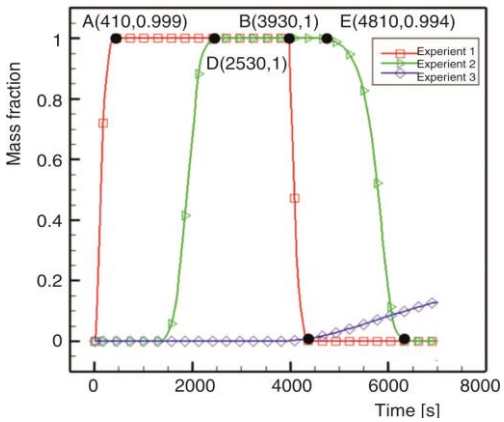

Figure 7. Change of mass fraction with time during the phase transition

To further illustrate the phase change process, this paper selects three measuring points for data analysis, as shown in fig. 7. The mass scores of measuring Point 1, measuring Point 2, and measuring Point 3 are all 0 at the initial time. This is because the heat transfer from the hot water flowing into the heat exchange tube takes a certain time, so the PCM has not yet begun to melt at the initial time. The heat in the thermal process increases, and the PCM at measuring Point 1 nearest to the heat exchange tube begins to melt [16]. When t = 410 seconds, the mass fraction becomes 1, indicating that the PCM gradually changes from a solid state to a liquid state. When t = 3930 seconds, cold water is injected into the tube and the heat release process begins. The mass fraction of the sample changes to 0 and the sample 1 begins to become a solid phase. The transformation from solid phase to liquid phase takes place after t = 2530 seconds, and the transformation from liquid phase to solid phase takes place after t = 4810 seconds. However, the phase transition process cannot be seen at the third measuring point, and the coexistence of solid and liquid occurs only at the last stage.

Conclusions

- The size of the fin structure has a great influence on the heat storage/release rate of the energy storage heat exchanger. In the area close to the tube wall of the heat exchange tube (measuring Point 1), the smaller the fin spacing, the thinner the thickness, the faster the phase change heat storage/dissipation speed, and the better heat transfer effect. In the central area of the PCM (measuring Point 2), the larger the fin spacing and thickness, the better the effect of phase transformation heat. The area near the outer wall has the minimum temperature change, and it is most difficult to complete heat storage and release.
- The finned tube energy storage heat exchanger near the tube wall of the heat exchange tube has a fast heat accumulation/release rate and good heat exchange effect. In the tube wall area close to the heat exchange tube (measuring Point 1) and phase change in the central area of the material (measuring Point 2), the PCM completely melts at t = 410 seconds and t = 2530 seconds, and the heat storage ends. When t = 3930 seconds and t = 4810 seconds, the PCM is completely solidified and the heat release ends.
- The use of energy storage heat exchangers with gradual fin thickness and spacing is an effective way to improve the heat exchange efficiency of existing equipment. In addition, for the purpose of improving the heat exchange effect of the phase change edge area, the structure of the edge area can be changed or the form of heat exchange can be increased.

Acknowledgment

The present work has been supported by the National Natural Science Foundation of China under the grant of 51906163, the Doctoral Starting Foundation of Liaoning Province (20180540120), the Natural science foundation of Liaoning Province (20180550472 and 2021-MS-270), the Liaoning province Department of Education fund (JL-2003 and JL-1914) and Shenyang Youth Innovation Support Project (RC190342).

References

[1] Liu, Y. K., *et al.*, Numerical Study on Performance Enhancement of Phase Change Heat Storage Unit (in Chinese), *Energy Storage Science and Technology*, *3* (2014), 3, pp. 197-202
[2] Song, X. N., *et al.*, Numerical Simulation of the Melting Process of the Phase Change Material Outside the Finned Tube (in Chinese), *Journal of Jiangsu University (Natural Science Edition)*, *38* (2017), 1, pp. 37-41
[3] Du, X. S., *et al.*, Flame-retardant and Solid-solid Phase Change Composites Based on Dopamine-Decorated BP Nanosheets/Polyurethane for Efficient Solar-to-thermal Energy Storage, *Renewable Energy*, *164* (2021), Feb., pp. 1-10
[4] Li, Y. H., *et al.*, Experimental Study on the Performance of Tube-Fin Phase Change Heat Accumulators, *Renewable Energy*, *32* (2014), 5, pp. 574-578
[5] Mat, S., *et al.*, Enhance Heat Transfer for PCM Melting in Triplex Tube with Internal-External Fins, *Energy Conversion and Management*, *74* (2013), Oct., pp. 223-236
[6] Al-Abidi, A. A., *et al.*, Numerical Study of PCM Solidification in a Triplex Tube Heat Exchanger with Internal and External Fins, *International Journal of Heat and Mess Transfer*, *61* (2013), June, pp. 684-695
[7] Tao, Y. B., *et al.*, Numerical Study on Performance of Molten Salt Phase Change Thermal Energy Storage System with Enhanced Tubes, *Solar Energy*, *86* (2012), 5, pp. 1155-1163
[8] Ismail, K. A. R., *et al.*, Numerical and Experimental Study on the Solidification of PCM around a Vertical Axially Finned Isothermal Cylinder, *Applied Thermal Engineering*, *21* (2001), 1, pp. 53-77
[9] Dai, Q. B., *et al.*, Experimental Study on the Heat Transfer Characteristics of Finned Tube Heat Accumulators with Solid-liquid Phase Change (in Chinese), *Building Thermal Ventilation and Air Conditioning*, *36* (2017), 8, pp. 35-38
[10] Gui, X., *et al.*, Influence of Void Ratio on Phase Change of Thermal Energy Storage for Heat Pipe Receiver, *Journal of Engineering Thermophysics*, *25* (2016), 2, pp. 275-287

[11] Jiang, J., *et al.*, Thermal Effect of Welding on Mechanical Behavior of High-Strength Steel, *Journal of Materials in Civil Engineering*, *33* (2021), 8, 04021186
[12] Malan, D.J., *et al.*, Solar Thermal Energy Storage in Power Generation Using Phase Change Material with Heat Pipes and Fins to Enhance Heat Transfer, *Energy Procedia*, 69 (2015), May, pp. 925-936
[13] Lu, H. W., *et al.*, Evaluating the Global Potential of Aquifer Thermal Energy Storage and Determining the Potential Worldwide Hotspots Driven by Socio-Economic, Geo-Hydrologic and Climatic Conditions, *Renewable & Sustainable Energy Reviews*, 112 (2019), Sept., pp. 788-796
[14] Sui, M. H., *et al.*, Temperature of Grinding Carbide with Castor Oil-Based MoS2 Nanofluid Minimum Quantity Lubrication, *Journal of Thermal Science and Engineering Applications*, 2021 (13), 5, pp. 1-30
[15] Zuo, X., *et al.*, The Modeling of the Electric Heating and Cooling System of the Integrated Energy System in the Coastal Area, *Journal of Coastal Research*, 103(2020), sp1, 1022
[16] Wang, B., *et al.*, Changes in the Thermal Stability and Structure of Protein from Porcine Longissimus Dorsi Induced by Different Thawing Methods, *Food Chemistry*, 316 (2020), June, pp. 126375-126375

Paper submitted: Apryl 1, 2021
Paper revised: July 3, 2021
Paper accepted: July 8, 2021